M&C 2017 - International Conference on Mathematics & Computational Methods Applied to Nuclear Science & Engineering, Jeju, Korea, April 16-20, 2017, on USB (2017)

Gyrokinetic simulations of electrostatic microinstabilities and turbulence with bounce-averaged kinetic electrons for shaped tokamak plasmas[1]

Lei Qi[1], Jaemin Kwon[1], T.S. Hahm[1,2], Sumin Yi[1]

[1]*National Fusion Research Institute, Daejeon 169-148, South Korea*
[2r]*Department of Nuclear Engineering, Seoul National University, Seoul 151-742, South Korea*
qileister@nfri.re.kr

Abstract - *Nonlinear bounce-averaged kinetic theory[B. H. Fong and T. S. Hahm, Phys. Plasmas 6, 188 (1999)] is used for magnetically trapped electrons for the purpose of achieving efficient gyrokinetic simulations of Trapped Electron Mode (TEM) dominant microturbulence transport in shaped tokamak plasmas. Bounce-averaged kinetic equations extended to shaped plasma equilibria are implemented to a global nonlinear gyrokinetic code, Gyro-Kinetic Plasma Simulation Program (gKPSP)[J. M. Kwon et al., Nucl. Fusion 52, 013004 (2012)]. The newly implemented code gKPSP is then benchmarked. With bounce-averaged gyrokinetic gKPSP simulation, stabilizing effects of elongation on both ITG and TEM can be understood in terms of magnetic flux expansion leading to the effective temperature gradient $R/L_T(1-E')$[P. Angelino et al., Phys. Rev. Lett. 102, 195002 (2009)] and poloidal wave length contraction at low field side resulting in the effective poloidal wave number $k_\theta\rho_i/\kappa$. Investigation of collisional effects on TEM using gKPSP demonstrates the parameter dependence of density gradient and electron temperature gradient. In nonlinear gKPSP simulations, plasma elongation is shown to reduce both electron and ion heat conductivities.*

I. INTRODUCTION

Microturbulence evolved from drift wave instabilities is believed to drive anomalous heat and particle transport in magnetic fusion plasmas, with Ion Temperature Gradient (ITG) mode and Trapped Electron Mode (TEM) being considered as primary candidates.

Gyrokinetic simulations are the most widely used and mature tools for the study of microturbulence[1]. Following pioneering works using conventional perturbation theory[2] or Hamiltonian approach in a simple geometry[3], firm theoretical foundations for nonlinear gyrokinetic simulations have been established by developments of modern gyrokinetics based on the phase space Lagrangian Lie perturbation method in a toroidal geometry[4]. Most gyrokinetic simulations of microturbulence reported in published literatures so far focus on either pure ITG or TEM[5]. Gyrokinetic simulations of nonlinear coupling of ITG-TEM are still relatively rare. One reason is that in the investigation of ITG-TEM microturbulence, one has to include both kinetic ions and trapped electrons, which require significant increases of computational resources compared to gyrokinetic simulations with adiabatic electrons.

In order to investigate ITG-TEM microturbulence more efficiently, especially to reduce computational resources required by kinetic trapped electrons, we use bounce-averaged kinetic theory in this work. Among other assumptions, the gyrokinetic theory assumes $\omega \ll \Omega_i$, where ω is frequency of interest, Ω_i is ion cyclotron frequency. With an additional assumption of $\omega \ll \omega_b$ (ω_b the bounce frequency), gyrokinetic equations can be reduced to bounce-averaged kinetic equations. In particular, the one developed by Fong and Hahm[6] retains full banana orbit width effect and addresses ion particle density calculations from bounce center distribution functions (i.e. pull-back transform) systematically. Bounce-averaged kinetic theory provides an efficient kinetic model for fast ITG-TEM turbulence simulation with realistic ion to electron mass ratio.

Plasma shaping, on the other hand, has considerable effects on the performance of tokamaks. Various tokamak experiments show that the energy confinement time τ_E significantly improves with increasing plasma shaping. In the past decades, there have been efforts to understand plasma shaping effects on turbulence and transport with analytic theories, gyrokinetic simulations and via experiments.[7] The most closely related work to ours is the one by P. Angelino on ITG[8].

In this paper, the bounce-averaged kinetic theory is extended from a toroidal geometry with circular magnetic flux surfaces to shaped plasmas and implemented into a global δf gyrokinetic Particle-In-Cell(PIC) code, gKPSP[9] for fast ITG-TEM simulations. The rest of this paper is organized as follows. In Sec. II, bounce-averaged kinetic description for shaped tokamak plasmas is presented. In Sec. III, plasma elongation effects on ITG-TEM are revisited by utilizing global gKPSP simulations. Collisional effects on ITG-TEM microinstability is investigated in Sec. IV. In Sec. V plasma elongation effects on ITG-TEM microturbulence transport is discussed. Conclusions are finally given, and future work is also discussed in Sec. VI.

II. BOUNCE-AVERAGED KINETIC DESCRIPTION OF TRAPPED ELECTRONS FOR SHAPED TOKAMAK PLASMAS

Starting from nonlinear electrostatic bounce-averaged kinetic theory for circular tokamak plasmas by Fong and Hahm[6], we extend the bounce-averaged kinetic equations to include plasma shaping parameters in this section.

For an MHD equilibrium that satisfies Grad-Shafranov

[1]Notice: this manuscript is a work of fiction. Any resemblance to actual articles, living or dead, is purely coincidental.

equation, we keep only three shaping parameters, the elongation κ, triangularity δ, and Shafranov shift Δ. With the assumption of relatively low triangularity, we obtain the following approximate MHD equilibrium characterized by

$$\begin{aligned} R &= R_0\left(1-\Delta+\varepsilon\cos\theta-\varepsilon\delta\sin^2\theta\right) \\ Z &= R_0\kappa\varepsilon\sin\theta, \end{aligned} \tag{1}$$

For this magnetic flux geometry of shaped plasmas, safety factor q and pitch angle κ_p of bounce motion are given by

$$q\left(\varepsilon,\kappa,\delta,\Delta\right)=\frac{\kappa B_0R_0^2}{8\psi_0}\left(1+2\Delta+\frac{\varepsilon^2+\delta\epsilon}{2}\right), \tag{2}$$

$$\kappa_p^2\left(\varepsilon,\kappa,q,\Delta\right)=\frac{K_0-\mu B_0\left(1+\Delta-\varepsilon+\frac{\kappa^2}{2q^2}\varepsilon^2\right)}{2\mu B_0\varepsilon\left(1+\Delta-\varepsilon+\frac{\kappa^2}{2q^2}\varepsilon^2\right)}, \tag{3}$$

where μ is magnetic moment, K_0 is the numerical value of total particle energy. With deeply trapped approximation, $\kappa_p \ll 1$, bounce-averaged flux and action-angle coordinates $(\beta,\alpha,\Psi,I,\mu)$ are expressed as,

$$\begin{aligned} \beta &= \psi_p, \\ \alpha &= \zeta-q\left(\varepsilon,\kappa,\delta,\Delta\right)\theta, \\ \Psi &= \pi+\mathrm{sgn}\left(v_\parallel\right)\left[\arcsin\left(\frac{\sin\left(\theta/2\right)}{\kappa_p}\right)+\pi/2\right], \\ I &\simeq 2qR_0\sqrt{m\varepsilon\mu B_0}\kappa_p^2, \end{aligned} \tag{4}$$

where ζ is toroidal angle, and m is mass, $v_\parallel$ is the velocity component parallel to magnetic field.

For the completeness of the bounce-averaged kinetic theory for shaped tokamak plasmas, one can find more detailed explanations in Ref.[10] on the bounce-averaged Hamiltonian H_0 and Vlasov equation, kinetic equations of motion and the gyrokinetic field equation for ITG-TEM turbulence. This bounce-averaged kinetic model was implemented into the gyrokinetic code gKPSP[9] and benchmarked with linear ITG-TEM and Rosenbluth-Hinton residual zonal flow in Ref. [10].

III. REVISITING ELONGATION EFFECTS ON ITG-TEM

We proceed to investigate the roles of plasma shaping parameters in ITG-TEM microinstabilities, especially elongation effects in this section.

1. Effective temperature gradient for ITG in elongated plasmas

Here we adopt the Cyclone parameters[10]. For convenience of interpretation, toroidal mode number is converted to poloidal wave number through $k_\theta = nq/r$. By fixing $R/L_n = 2.22$, scans in both R/L_T and κ have been performed. Growth rate of the most linearly unstable mode selected in a scan of n is measured and plotted as a function of R/L_T and κ in Fig. 1 (left figure). Stabilizing effect of elongation on ITG mode can be seen from the figure for all values of R/L_T, which is consistent with other published literatures. It has been demonstrated in Ref. [8] that global ITG mode feels an average temperature gradient, and the effective scale length of the average temperature gradient is modified to be $R/L_T(1-E')$ with $E = r(\kappa-1)/(\kappa+1)$. In terms of this effective temperature gradient, the five curves in Fig. 1 (left figure) fall on the same curve. The same result is also obtained from gKPSP as shown in Fig. 1 (right figure).

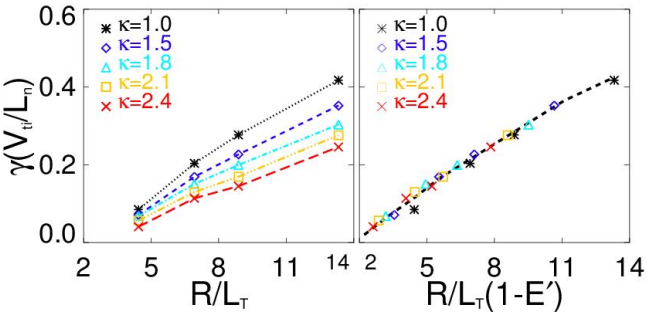

Fig. 1. Growth rate of the most linearly unstable ITG mode in a scan of $k_\theta\rho_i$, as a function of κ and R/L_T (left figure) and the effective temperature gradient $R/L_T\,(1-E')$ (right figure).

2. Role of elongation in linear ITG-TEM drive, the effective poloidal wave number

Next, we extend the study to elongation effects on linear ITG-TEM drive. Previous Cyclone parameters are adopted again with $\eta_i = \eta_e = 3.118$, that is $R/L_n = 2.22$ and $R/L_{T_i} = R/L_{T_e} = 6.92$. Elongation takes values of $\kappa = 1.0$(circular), 1.25 and 1.5. Real frequency of ITG-TEM from gKPSP simulations are plotted as a function of poloidal wave number in the left figure of Fig. 2. It can be seen from the figure that not only values of frequency are changed, but also transition trends from ITG to TEM are varied for different elongations. Higher elongation results in lower frequency and higher transition poloidal wave number $k_\theta\rho_i$, at which ITG mode transits to TEM.

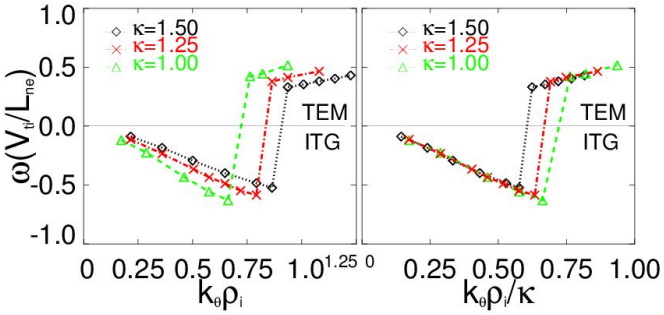

Fig. 2. Real frequency of ITG-TEM mode as a function of $k_\theta\rho_i$ (left figure) and the effective poloidal wave number $k_\theta\rho_i/\kappa$ (right figure) for $R/L_n = 2.22$ and $R/L_{T_i} = R/L_{T_e} = 6.92$. Different elongations of $\kappa = 1.0, 1.25, 1.5$ are plotted..

Note that in the previous subsection, we discussed ITG mode "feels" an effective temperature gradient due to the elongation-induced magnetic flux expansion. When considering dispersion relation of the global ITG-TEM mode in the elongated plasma, we assume that elongation also induces a contraction in poloidal wave length by a factor of $1/\kappa$ at low field side. Therefore, under this assumption, by introducing an effective poloidal wave number $k_\theta\rho_i/\kappa$, results in the left figure of Fig. 2 can be better understood. In terms of $k_\theta\rho_i/\kappa$, the ITG-TEM frequency in the left figure of Fig. 2 corresponding to the three values of elongation fall on the same curve in both ITG and TEM branches as shown in the right figure of Fig. 2. This result demonstrates the correctness of the assumption of effective poloidal wave number.

Now, we proceed to give a physical interpretation of the effective poloidal wave number. From the relevant eikonal expression in a general toroidal geometry in Ref. [2], a more general expression for the poloidal wave number is given by $k_\theta^{eff}(\theta) = \frac{nB}{RB_\theta} \simeq \frac{nB_t}{RB_\theta}$. Since ITG-TEM eigenmodes are localized around $\theta = 0$, we have $k_\theta^{eff}(\theta = 0) = \frac{nq}{r}\frac{1}{\kappa\left(1+\frac{1}{2}\varepsilon^2\right)} \approx \frac{nq}{r}\frac{1}{\kappa} = \frac{k_\theta}{\kappa}$. The derivation demonstrates the effective poloidal wave number is what ITG-TEM mode actually feels due to plasma elongation, and also explains the observations in Ref. [8] and our gKPSP simulations.

IV. GKPSP SIMULATIONS WITH COLLISIONS AND NONLINEAR TURBULENCE TRANSPORT

In previous sections, linear gyrokinetic simulations with bounce-averaged kinetic trapped electrons in gKPSP were proved to work properly, however the simulation with collision or the nonlinear simulations of the turbulence is not confirmed. Since the bounce-averaged technique is applied to kinetic trapped electrons, however trapped electrons or passing electrons could cross the trap-passing boundary due to collision or nonlinear fluctuations, nonlinear ITG-TEM simulations or simulations with a finite collisionality can only be achieved in a correct way only if trapped electrons population and passing electrons population are connected dynamically and smoothly. This has been numerically achieved in gKPSP code, and results of collisional ITG-TEM mode as well as ITG-TEM driven turbulence are presented in this section.

1. Collisional ITG-TEM

Cyclone parameters in Sec. 3.1 are adopted again in this section. Scans are performed for various poloidal wave numbers without collisions and with collisions $\nu_* = 0.135$, as shown in the left figure of Fig. 3. It can be seen from the figure that ITG growth rates are decreased slightly by the strong collision, while TEM is strongly suppressed by the collision, which is consistent with other published literatures.

As TEM can be suppressed by collisions due to the detrapping processes, it is interesting to investigate the dependence of the growth rate of TEM on collisionality. Since TEM can be driven by the density gradient and electron temperature gradient respectively, it is necessary to test collision effect on both density gradient driven and electron temperature gradient driven TEMs, which is shown in the right figure of Fig.

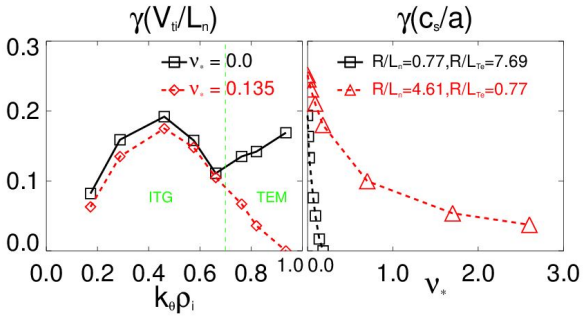

Fig. 3. Left figure: growth rates of ITG-TEM cases from gKPSP without collision (black) and with collision $\nu_* = 0.135$ (red). Right figure: growth rates of TEM cases from gKPSP as a function of collisionality ν_* for two cases $R_0/L_n = 0.77$, $R_0/L_{Te} = 7.69$ (black square) and $R_0/L_n = 4.61$, $R_0/L_{Te} = 0.77$ (red triangle).

3. Cyclone parameters with $R_0/L_{Ti} = 0.0$, $T_e/T_i = 2.0$ are adopted. For the case depicted as the black line in the figure, $R_0/L_n = 0.77$, $R_0/L_{Te} = 7.69$ indicating mainly electron temperature gradient driven TEM, the mode is quickly and completely suppressed as collisionality increases. For the case shown as red line in the figure, $R_0/L_n = 4.61$, $R_0/L_{Te} = 0.77$ mainly density gradient driven TEM, the mode is stabilized but not completely, even at very high collisionalities. Thus at the high collisonalities, the density gradient driven TEM can be still unstable. This finding from gKPSP confirms C. Angioni's simulations[11] and observations in experiments operating at high collisionality.

2. Elongation effect on TEM dominated turbulence transport

We proceed to study nonlinear bounce-averaged gKPSP simulations of TEM dominant turbulence transport in elongated plasmas. We carried out simulations with the following parameters: $R_0 = 1.86m$, $B_0 = 1.91T$, $T_e = 2.5kev$, $n_e = 1.46 \times 10^{20}m^{-3}$, $R_0/L_{Te} = 6.9$, $R_0/L_{Ti} = 2.2$, $R_0/L_n = 2.2$, $a/\rho_i = 250$, $a/R_0 = 0.358$, $T_i = T_e$, $m_i/m_e = 1836$, and the safety factor $q = 0.58 + 1.09r/a + 1.09(r/a)^2$, with magnetic shear, $s = d\ln q/d\ln n = 0.78$ at $r = 0.5a$. The electron(ion) heat flux $q_e(q_i)$ is represented by the effective heat conductivity $\chi_e(\chi_i)$ through the relation $q_j = n_j\chi_j\nabla T_j$ with j being e or i. Since electron heat flux is mostly carried by trapped electrons, here n_e is the trapped electron density. $q_j = \int d^3v(1/2v^2v_E\delta f_j)$ with v_E being the radial component of the gyroaveraged $E \times B$ drift, and δf_j is the kinetic electron (or ion) distribution function. Electron (ion) heat conductivity is normalized to gyroBohm diffusivity $\chi_{GB} = \rho_i^2 v_i/a$. In Fig. 4, gKPSP simulation results of χ_i(left) and χ_e(right) for elongations of $\kappa = 1.0$(black) and $\kappa = 1.8$(red) are presented in terms of time history.

From the figure, it can be seen that in these parameters, the level of electron heat conductivity is much higher than the level of ion heat conductivity, which demonstrates that this case is TEM dominant and consistent with the linear results. In the figure, it is also shown that the elongation can decrease

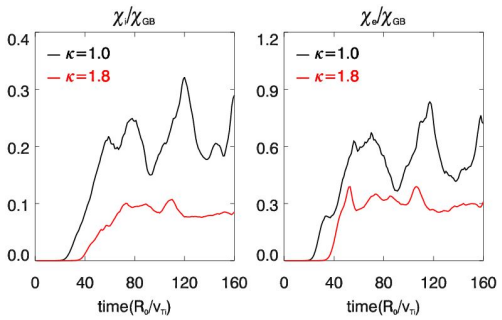

Fig. 4. Left figure: Ion heat conductivity χ_i normalized to gyroBohm diffusivity χ_{GB} as a function of time for elongation $\kappa = 1.0$ (black) and $\kappa = 1.8$ (red). Right figure: Electron heat conductivity χ_e normalized to gyroBohm diffusivity χ_{GB} as a function of time for elongation $\kappa = 1.0$ (black) and $\kappa = 1.8$ (red).

both the electron and ion heat conductivities, which indicates that the elongation has stabilizing effect on this ITG-TEM driven turbulence.

V. CONCLUSIONS AND FUTURE WORK

Bounce-averaged kinetic theory for shaped tokamak plasmas was implemented into the gyrokinetic code gKPSP for fast ITG-TEM simulations, from which we have obtained the following conclusions. 1) Stabilizing effects of elongation on both ITG and TEM can be understood in terms of magnetic flux expansion leading to the effective temperature gradient $R/L_T(1-E')$ and poloidal wave length contraction at low field side resulting in the effective poloidal wave number $k_\theta\rho_i/\kappa$. 2) collisional effects on TEM depend on parameters of density gradient and electron temperature gradient. 3) plasma elongation can stabilize both electron and ion heat conductivity in TEM dominant turbulence transport. For the future work, investigation of saturation mechanism of TEM dominant turbulence is planned, especially to understand the stabilizing effect of elongation on ITG-TEM driven turbulence, such as the enhancement of residual zonal flow, etc. The characters of TEM-driven turbulent transport in low collisionality regime will be also studied in future.

VI. ACKNOWLEDGMENTS

This research was supported by the R&D Program through National Fusion Research Institute (NFRI) funded by the Ministry of Science, ICT and Future Planning of the Republic of Korea (NFRI-EN1641).

REFERENCES

1. Z. LIN, T. S. HAHM, W. W. LEE, W. M. TANG, and R. B. WHITE, "Turbulent transport reduction by zonal flows: Massively parallel simulations," *Science*, **281**, 1835 (1998).
2. E. A. FRIEMAN and L. CHEN, "Nonlinear gyrokinetic equations for low-frequency electromagnetic waves in general plasma equilibria," *Phys. Fluids*, **25**, 502 (1982).
3. T. S. HAHM, W. W. LEE, and A. BRIZARD, "Nonlinear gyrokinetic theory for finite-beta plasmas," *Phys. Fluids*, **31**, 1940 (1988).
4. T. S. HAHM, "Nonlinear gyrokinetic equations for tokamak microturbulence," *Phys. Fluids*, **31**, 2670 (1988).
5. Y. XIAO and Z. LIN, "Turbulent transport of trapped-electron modes in collisionless plasmas," *Phys. Rev. Lett*, **103**, 085004 (2009).
6. B. H. FONG and T. S. HAHM, "Bounce-averaged kinetic equations and neoclassical polarization density," *Phys. Plasmas*, **6**, 188 (1999).
7. G. REWOLDT, W. M. TANG, and M. CHANCE, "Electromagnetic kinetic toroidal eigenmodes for general magnetohydrodynamic equilibria," *Phys. Fluids*, **25**, 480 (1982).
8. P. ANGELINO, X. GARBET, L. VILLARD, A. BOTTINO, S. JOLLIET, P. GHENDRIH, V. GRANDGIRARD, B. F. MCMILLAN, Y. SARAZIN, G. DIFPRADALIER, and T. M. TRAN, "Role of plasma elongation on turbulent transport in magnetically confined plasmas," *Phys. Rev. Lett.*, **102**, 195002 (2009).
9. J. M. KWON, S. YI, T. RHEE, P. H. DIAMOND, K. MIKI, T. S. HAHM, J. Y. KIM, O. D. GURCAN, and C. MCDEVITT, "Analysis of symmetry breaking mechanisms and the role of turbulence self-regulation in intrinsic rotation," *Nucl. Fusion*, **52**, 013004 (2012).
10. L. QI, J. M. KWON, T. S. HAHM, and G. JO, "Gyrokinetic simulations of electrostatic microinstabilities with bounce-averaged kinetic electrons for shaped tokamak plasmas," *Nucl. Fusion*, **23**, 062513 (2016).
11. C. ANGIONI, A. G. PEETERS, F. JENKO, and T. DANNERT, "Collisionality dependence of density peaking in quasilinear gyrokinetic calculations," *Phys. Plasmas*, **12**, 112310 (2005).